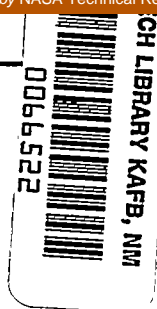


NACA TN 3588



# NATIONAL ADVISORY COMMITTEE FOR AERONAUTICS

TECHNICAL NOTE 3588

SUMMARY OF LAMINAR-BOUNDARY-LAYER SOLUTIONS FOR  
WEDGE-TYPE FLOW OVER CONVECTION- AND  
TRANSPIRATION-COOLED SURFACES

By John N. B. Livingood and Patrick L. Donoughe

Lewis Flight Propulsion Laboratory  
Cleveland, Ohio



Washington

December 1955

AFM 5

TECH LIBRARY

TECH LIBRARY KAFB, NM





## NATIONAL ADVISORY COMMITTEE FOR AERONAUTICS

## TECHNICAL NOTE 3588

SUMMARY OF LAMINAR-BOUNDARY-LAYER SOLUTIONS FOR WEDGE-TYPE FLOW  
OVER CONVECTION- AND TRANSPIRATION-COOLED SURFACES

By John N. B. Livingood and Patrick L. Donoughe

## SUMMARY

A summary of exact solutions of the laminar-boundary-layer equations for wedge-type flow, useful in estimating heat transfer to such arbitrarily shaped bodies as turbine blades, is presented. The solutions are determined for small Mach numbers and a Prandtl number at the wall of 0.7; ranges of mainstream pressure gradients and rates of coolant flow through a porous wall are considered for the following cases: (1) small temperature changes in the boundary layer along a constant- and along a variable-temperature wall, and (2) large temperature changes in the boundary layer along a constant-temperature wall.

Dimensionless forms of heat-transfer and friction parameters and boundary-layer thicknesses are tabulated. The results indicate that coolant emission and increased stream-to-wall temperature ratios diminished the friction and heat transfer for a constant wall temperature. For a variable wall temperature with small temperature differences in the boundary layer, the friction was unaffected, but the heat transfer was greatly increased for increased wall-temperature gradient. Heat-transfer results in the literature reveal that transpiration cooling is much more effective for Prandtl numbers of the order of 5.0 than for 0.7.

## INTRODUCTION

The cooling of structural parts in propulsion systems such as gas-turbine blades, combustion-chamber walls, and rocket nozzles has become increasingly important with the growing demand for higher-powered and more efficient systems. Such cooling may be accomplished by either convection or transpiration methods. Convection cooling is obtained by passing cooling air along the coolant side of the wall; transpiration cooling is accomplished by forcing the coolant through a permeable wall. Methods previously used to predict heat transfer had to be extended to include transpiration cooling for the different types of application. The NACA Lewis laboratory has initiated a program to extend such methods in the laminar-flow region.

3791

CV-1

Exact solutions of laminar-boundary-layer equations for wedge-type flow have been found useful in predicting laminar heat transfer to bodies with impermeable walls (ref. 1). (Wedge-type flow is flow for which the mainstream velocity is proportional to a power of the distance from the stagnation point.) However, only a few solutions for heat transfer existed for transpiration-cooled wedges (ref. 2); these were determined for conditions of constant wall temperature, constant fluid properties, and a Prandtl number of unity. In order to apply this method to the cooling of such structural parts of propulsion systems as turbine blades, wedge solutions were required for conditions applying to such components. These conditions include the simultaneous effects of flow through a porous wall, large pressure gradients in the mainstream, small Mach numbers, small temperature differences through the laminar boundary layer (constant property values or a stream-to-wall temperature ratio near unity), and large temperature differences through the laminar boundary layer (variable property values or stream-to-wall temperature ratios appreciably different from unity).

Exact solutions of the laminar-boundary-layer equations for a range of flows through a porous wall, for a range of pressure gradients, and for several stream-to-wall absolute temperature ratios are presented in references 3 to 5 for a Prandtl number at the wall of 0.7. In these solutions the wall temperature was assumed constant, and the range of stream-to-wall temperature ratios was chosen to include the cases both of constant property values and of property values that varied with powers of the absolute temperature. Wedge solutions are presented in reference 6 for constant property values and a variable wall temperature. Again the Prandtl number was chosen as 0.7. Solutions for isothermal impermeable flat plates are contained in reference 7 for various Prandtl numbers; the results are extended to wedge-type flow in reference 8. Solutions for impermeable wedges that illustrate the effect of Prandtl number, pressure gradient, and surface temperature variation are presented and summarized in reference 9. Reference 10 presents analytical heat-transfer results for an isothermal permeable flat plate with fluids of different Prandtl numbers.

Wedge solutions can be utilized to obtain approximate information on heat transfer to bodies of arbitrary shape. A first approximation can be obtained by stipulating that the heat-transfer coefficient at any location on a body of arbitrary cross section is identical with the heat-transfer coefficient on a wedge for which, at the same distance from the stagnation point, the stream velocity and the stream-velocity gradient are the same as those on the arbitrarily shaped body. (Such use of wedge solutions is made for an impermeable cylinder in ref. 1. The method is described for permeable bodies in appendix C of ref. 11.) This approximation satisfies local stream conditions only, and does not properly account for the development of the boundary layer ahead of the point under consideration. Taking into account the development of the boundary layer



$C_{f,\infty}$	local skin-friction coefficient based on properties at stream temperature, $\frac{\tau_w}{\frac{\rho_\infty U_\infty^2}{2}}$
$c_p$	specific heat at constant pressure
$Eu$	Euler number, $\frac{-x \frac{\partial p}{\partial x}}{\rho_\infty U_\infty^2}$ ; $U_\infty = Cx^{Eu}$ for wedge-type flow
$f$	dimensionless stream function, $\rho_w \psi / \sqrt{U_\infty \rho_w \mu_w x}$
$f', f'', f'''$	first, second, and third derivatives of $f$ with respect to $\eta$
$H$	local heat-transfer coefficient
$k$	thermal conductivity
$Nu$	local Nusselt number, $Hx/k_w$
$n$	wall-temperature-gradient parameter, $\frac{x}{T_w - T_\infty} \frac{dT_w}{dx}$ ; $T_w - T_\infty = Bx^n$
$Pr$	Prandtl number, $\frac{c_p \mu}{k}$
$p$	static pressure
$Re$	local Reynolds number, $\frac{U_\infty x}{\nu_w}$
$T$	temperature
$U_\infty$	fluid velocity at edge of boundary layer
$u$	fluid velocity in boundary layer parallel to wall
$v$	fluid velocity in boundary layer normal to wall

3791

- x distance along surface
- y distance normal to surface
- $\alpha$  exponent of temperature for specific heat,  $c_p \propto T^\alpha$
- $\delta$  boundary-layer thickness
- $\delta^*$  displacement-layer thickness,  $\int_0^\infty \left(1 - \frac{\rho u}{\rho_\infty U_\infty}\right) dy$
- $\delta_c$  convection-layer thickness,  $\int_0^\infty \frac{\rho u}{\rho_\infty U_\infty} \left(\frac{T - T_\infty}{T_w - T_\infty}\right) dy$
- $\delta_i$  momentum-layer thickness,  $\int_0^\infty \frac{\rho u}{\rho_\infty U_\infty} \left(1 - \frac{u}{U_\infty}\right) dy$
- $\delta_t$  thermal-layer thickness,  $\int_0^\infty \frac{T - T_\infty}{T_w - T_\infty} dy$
- $\epsilon$  exponent of temperature for thermal conductivity,  $k \propto T^\epsilon$
- $\eta$  dimensionless boundary-layer coordinate,  $y \sqrt{\frac{\rho_w U_\infty}{\mu_w x}}$
- $\theta$  temperature-difference ratio,  $\frac{T - T_w}{T_\infty - T_w}$
- $\theta', \theta''$  first and second derivatives of  $\theta$  with respect to  $\eta$
- $\mu$  absolute viscosity of fluid
- $\nu$  kinematic viscosity,  $\mu/\rho$
- $\rho$  density of fluid
- $\tau$  shear stress
- $\psi$  stream function

$\omega$  exponent of temperature for viscosity,  $\mu \propto T^\omega$

Subscripts:

w wall

$\infty$  mainstream, outside boundary layer

### ANALYSIS

Solutions of the laminar-boundary-layer equations for small temperature changes in the boundary layer along constant- and variable-temperature walls and for large temperature changes in the boundary layer along a constant-temperature wall are discussed. Details of the analyses and calculation methods are not contained herein, but are available in references 3 to 6.

#### Boundary-Layer Equations

The equations of the laminar boundary layer for steady-state flow of a viscous fluid with heat transfer are as follows:

Momentum:

$$\rho u \frac{\partial u}{\partial x} + \rho v \frac{\partial u}{\partial y} = \frac{\partial}{\partial y} \left( \mu \frac{\partial u}{\partial y} \right) - \frac{\partial p}{\partial x} \quad (1)$$

Continuity:

$$\frac{\partial}{\partial x} (\rho u) + \frac{\partial}{\partial y} (\rho v) = 0 \quad (2)$$

Energy: If the temperature differences between the wall and the mainstream are assumed large compared with temperature changes caused by compression and frictional heating, the energy equation may be written

$$\rho c_p \left( u \frac{\partial T}{\partial x} + v \frac{\partial T}{\partial y} \right) = \frac{\partial}{\partial y} \left( k \frac{\partial T}{\partial y} \right) \quad (3)$$

Equations (1) to (3) include transpiration cooling for the case when the same medium as that in the outside flow is used as coolant and the following boundary conditions are defined:

$$\left. \begin{aligned}
 &u = 0, v = v_w, \text{ and } T = T_w \text{ for } y = 0 \\
 &\text{and} \\
 &u \rightarrow U_\infty \text{ and } T \rightarrow T_\infty \text{ for } y \rightarrow \infty
 \end{aligned} \right\} \quad (4)$$

The property values  $\mu$ ,  $k$ ,  $c_p$ , and  $\rho$  appearing in the equations are assumed to be either constant or functions of temperature only.

Change of Variables

A transformation of the partial differential equations is accomplished by changing the independent variables  $x$  and  $y$  into new independent variables  $x$  and  $\eta$  where

$$\eta = y \sqrt{\frac{\rho_w U_\infty}{\mu_w x}} \quad (5)$$

In addition, the dependent variables  $u$ ,  $v$ , and  $T$  are replaced by the new dependent variables  $f$  and  $\theta$  (refs. 15 and 7), where

$$\left. \begin{aligned}
 f &= \frac{\rho_w \psi}{\sqrt{\rho_w \mu_w U_\infty x}} \\
 \theta &= \frac{T - T_w}{T_\infty - T_w}
 \end{aligned} \right\} \quad (6)$$

The continuity equation is satisfied by the stream function  $\psi$ , and hence

$$\left. \begin{aligned}
 \rho u &= \frac{\partial(\rho_w \psi)}{\partial y} \\
 \rho v &= - \frac{\partial(\rho_w \psi)}{\partial x}
 \end{aligned} \right\} \quad (7)$$

Application of these changes in variables to equations (1) to (3) results in a set of equations that, in principle, can be solved for two-dimensional flow about any arbitrary shape. For engineering purposes, however, obtaining such solutions is not feasible. As a consequence, exact solutions for wedge-type flow will be presented herein that can be used by the two methods explained in the INTRODUCTION to approximate heat transfer to bodies of arbitrary cross section.

3791

Ordinary Differential Equations for Small  
Stream-to-Wall Temperature Differences  
(Constant and Variable Wall Temperatures)

As already stated, for constant property values including density (small temperature differences), both constant and variable wall temperatures are considered herein. For variable wall temperature, it is assumed that the difference between the wall and stream temperatures is proportional to a power of the distance from the leading edge; that is,

$$T_w - T_\infty = Bx^n \quad (8)$$

where  $n$  and  $T_\infty$  are constants (refs. 16 to 18). Differentiation of equation (8) yields the following expression for the wall-temperature-gradient parameter:

$$n = \frac{x}{T_w - T_\infty} \frac{dT_w}{dx} \quad (9)$$

For wedge-type flow the stream velocity varies as a power function of the distance from the stagnation point measured along the surface:

$$U_\infty = Cx^m \quad (10)$$

It is customary to refer to the exponent  $m$  in this equation as Euler number. The Euler number can be expressed by the Bernoulli equation

$$Eu = \frac{-\frac{\partial p}{\partial x}}{\frac{\rho_\infty U_\infty^2}{x}} = \frac{x}{U_\infty} \frac{dU_\infty}{dx} \quad (11)$$

Assuming that  $f$  and  $\theta$  are functions of  $\eta$  only and using equations (5) to (11) transform equations (1) to (3) into the total differential equations:

$$f'''' = Eu f'^2 - \frac{Eu + 1}{2} f f'' - Eu \quad (12)$$

$$\theta'' = -\frac{Eu + 1}{2} Pr f \theta' - n Pr f' (1 - \theta) \quad (13)$$

with the boundary conditions

$$\left. \begin{aligned} f &= f_w, f' = 0, \text{ and } \theta = 0 \text{ for } \eta = 0 \\ \text{and} \\ f' &\rightarrow 1 \text{ and } \theta \rightarrow 1 \text{ for } \eta \rightarrow \infty \end{aligned} \right\} \quad (14)$$

Equation (13) is identical to equation (12) of reference 6 when the substitution  $Y = 1 - \theta$  is made, where  $Y = \frac{T - T_\infty}{T_w - T_\infty}$ .

The velocity at the surface ( $y = 0$ ) is

$$v_w = - \frac{Eu + 1}{2} \sqrt{\frac{\mu U_\infty}{\rho x}} f_w \quad (15)$$

The transformation, therefore, prescribes a certain variation of the cooling velocity  $v_w$  along the surface, since the function  $f_w$  has to be constant (independent of  $x$ ). Because the stream velocity is described by equation (10), the coolant velocity  $v_w$  is also proportional to some power of  $x$ , namely  $v_w \propto x^{\frac{Eu-1}{2}}$ . Reference 2 shows that such a variation of the coolant velocity leads to a constant wall temperature when heat transfer by conduction and radiation may be neglected. Only conduction along the wall, or radiation, or both may lead to the case of a wall-temperature variation if  $f_w$  is constant.

Ordinary Differential Equations for Large Stream-  
to-Wall Temperature Differences  
(Constant Wall Temperature)

In order to account for changes in the fluid properties, the following property variations with absolute temperature are employed:

$$\mu \propto T^{\omega}, k \propto T^{\epsilon}, c_p \propto T^{\alpha}, \rho \propto T^{-1} \quad (16)$$

Use of equations (16) and equations (5), (6), (7), (10), and (11) transforms equations (1) and (3) into the total differential equations:

3791

CV-2

$$\theta'' = -\frac{Eu+1}{2} Pr_w \left(\frac{T}{T_w}\right)^{\alpha-\epsilon} \theta' f - \epsilon \left(\frac{T_\infty}{T_w} - 1\right) \left(\frac{T}{T_w}\right)^{-1} \theta'^2 \quad (17)$$

$$f''' = Eu \left(\frac{T}{T_w}\right)^{-\omega} f'^2 - \frac{Eu+1}{2} \left(\frac{T}{T_w}\right)^{-\omega} f f'' - Eu \left(\frac{T_\infty}{T_w}\right)^{-1} \left(\frac{T}{T_w}\right)^{-\omega-1}$$

$$\frac{Eu+1}{2} \left(\frac{T_\infty}{T_w} - 1\right) \left(\frac{T}{T_w}\right)^{-\omega-1} f f' \theta' - \left(\frac{T_\infty}{T_w} - 1\right) \left(\frac{T}{T_w}\right)^{-1} f' \theta'' -$$

$$(\omega+2) \left(\frac{T_\infty}{T_w} - 1\right) \left(\frac{T}{T_w}\right)^{-1} f'' \theta' - \omega \left(\frac{T_\infty}{T_w} - 1\right)^2 \left(\frac{T}{T_w}\right)^{-2} f' \theta'^2 \quad (18)$$

The boundary conditions are

$$\left. \begin{aligned} f = f_w, f' = 0, \text{ and } \theta = 0 \text{ for } \eta = 0 \\ \text{and} \\ f' \rightarrow \frac{T_w}{T_\infty} \text{ and } \theta \rightarrow 1 \text{ for } \eta \rightarrow \infty \end{aligned} \right\} \quad (19)$$

The velocity at the surface is now given by

$$v_w = -\frac{Eu+1}{2} \sqrt{\frac{\mu_w U_\infty}{\rho_w x}} f_w$$

Boundary-Layer Thicknesses, Heat Transfer, and Friction

From equations (5) to (7) it follows that

$$\frac{\rho u}{\rho_w U_\infty} = f'$$

The specific-weight-flow ratio is therefore expressible as

$$\frac{\rho u}{\rho_\infty U_\infty} = f' \frac{T_\infty}{T_w} \quad (20)$$

and the velocity ratio is expressible as

$$\frac{u}{U_\infty} = f' \frac{T}{T_w} \quad (21)$$

From equations (5) to (7), (20), and (21), and the definitions of the boundary-layer thicknesses given in the SYMBOLS, dimensionless forms of the displacement, momentum, convection, and thermal boundary-layer thicknesses may be expressed as follows:

$$\frac{\delta^*}{x} \sqrt{\text{Re}} = \int_0^\infty \left( 1 - f' \frac{T}{T_w} \right) d\eta \quad (22)$$

$$\frac{\delta_i}{x} \sqrt{\text{Re}} = \frac{T_\infty}{T_w} \int_0^\infty f' \left( 1 - \frac{T}{T_w} f' \right) d\eta \quad (23)$$

$$\frac{\delta_c}{x} \sqrt{\text{Re}} = \frac{T_\infty}{T_w} \int_0^\infty f' (1 - \theta) d\eta \quad (24)$$

$$\frac{\delta_t}{x} \sqrt{\text{Re}} = \int_0^\infty (1 - \theta) d\eta \quad (25)$$

Equating the convective heat transfer  $H(T_\infty - T_w)$  to the conductive heat transfer  $k_w(\partial T/\partial y)_w$  and using equations (5) and (6) yield the dimensionless form of the heat-transfer parameter

$$\frac{\text{Nu}}{\sqrt{\text{Re}}} = \theta'_w \quad (26)$$

With the wall shear stress given by

$$\tau_w = \left( \mu \frac{\partial u}{\partial y} \right)_w \quad (27)$$

and friction coefficients defined as

3791

CV-2 back

$$C_{f,w} = \frac{\tau_w}{\frac{\rho_w U_\infty^2}{2}}$$

or

$$C_{f,\infty} = \frac{\tau_w}{\frac{\rho_\infty U_\infty^2}{2}}$$

the dimensionless forms of the friction parameter are

$$\frac{C_{f,w} \sqrt{Re}}{2} = f_w''$$

or

$$\frac{C_{f,\infty} \sqrt{Re}}{2} = f_w'' \frac{T_\infty}{T_w} \quad (28)$$

#### Assumptions for Numerical Calculations

The numerical solutions were obtained for a Prandtl number at the wall of 0.7 (appropriate for air), pressure variations represented by values of  $Eu$  of 0, 1/2, and 1, flow rates through the porous wall represented by values of  $f_w$  of 0, -1/2, and -1, and wall-temperature variations represented by values of  $n$  from the value corresponding to a zero wall-temperature gradient to unity.

For large temperature differences, the exponents in equation (16) are required. These exponents, determined by logarithmic plots of the properties of air against temperature (600° to 2400° F) using the property values given in reference 19, are as follows:

Exponent in viscosity-temperature relation, $\omega$ . . . . .	0.7
Exponent in thermal-conductivity - temperature relation, $\epsilon$ . . . . .	0.85
Exponent in specific-heat - temperature relation, $\alpha$ . . . . .	0.19

#### RESULTS AND DISCUSSION

The heat-transfer and friction parameters and boundary-layer thicknesses are presented in table II. In addition, values of  $n$  that result

in  $\theta'_w = 0$  (for small temperature differences) and values of  $Eu$  that result in  $f''_w = 0$  (for constant wall temperature) are also given. Values of  $f$ ,  $\theta$ , and their derivatives may be obtained from references 4 to 6 except for cases where  $f_w = 0$ ,  $n = 0$ , and  $Eu < 0$ . For these cases, only  $f'$  and  $\theta$  are listed. Representative profiles are shown in figures 1 to 4 herein. Unless otherwise noted, the source of the distribution is given in table II.

### Boundary-Layer Profiles

Figure 1 presents velocity distributions in the boundary layer. Parts (a), (c), and (e) are for the flat plate aligned with the mainstream ( $Eu = 0$ ); parts (b), (d), and (f) are for the plate perpendicular to the stream or stagnation flow ( $Eu = 1$ ). Figures 1(a) and (b) illustrate the effects of coolant emission or blowing through the porous wall for constant property values. Distributions for additional blowing rates are obtained from references 20 and 21.

Because equations (12) and (13) are independent, the distributions in figures 1(a) and (b) apply for either a constant or variable wall temperature and for all Prandtl numbers. Increasing coolant flow ( $|f_w|$  increasing) reduces the velocity at a given value of  $\eta$ ; this amounts to a reduction in local shear stress. The distribution for  $f_w = -1.2$  in figure 1(a) yields very small values for the velocity gradients (e.g.,  $f''(0) = 0.0033575$ ). When  $f_w = -1.23849$ , the velocity gradient at the wall becomes zero, according to reference 20.

The S-shape of the velocity profiles, undesirable with respect to stability, is quite marked in figure 1(a) for all nonzero values of  $f_w$ . Inspection of figure 1(b) for stagnation flow reveals that even for large values of blowing there is no inflection point inside the boundary layer. This stabilizing influence of the pressure gradient is discussed in considerable detail in reference 22.

Figures 1(c) and (d) show the effects of variable property values on the velocity distribution when the wall temperature is constant. The different values of  $T_\infty/T_w$  do not appreciably affect the shape when  $Eu = 0$ ; for stagnation flow ( $Eu = 1$ ), however, there is a marked effect of  $T_\infty/T_w$  on the distribution, which actually results in velocity overshoot ( $\frac{u}{U_\infty} > 1$ ) for  $T_\infty/T_w < 1$ . For the case of a favorable pressure gradient and a heated wall ( $Eu = 1$ ,  $T_\infty/T_w < 1$ ), the density is lowered so

that the flow inside the boundary layer is accelerated more than the external flow is accelerated by the pressure forces; overshoot results. For large temperature differences, the main stability criterion is  $\frac{\partial}{\partial y} \left( \rho \frac{\partial u}{\partial y} \right)$ . Figure 1(c) shows there are no inflection points inside the boundary layer regardless of temperature ratio.

Figures 1(e) and (f) illustrate the combined effects of a porous wall and variable property values for a constant wall temperature. The velocity gradients (and, hence, shear stress) are decreased by increasing  $T_\infty/T_w$  and  $|f_w|$ .

Comparison of the curves for  $Eu = 0$  with those for  $Eu = 1$  shows that in all cases the pressure gradient tends to reduce the boundary-layer thickness and to increase the shear stress.

Figure 2 contains plots of the temperature-difference ratio  $(T - T_w)/(T_\infty - T_w) = \theta$  against the dimensionless boundary-layer coordinate  $\eta$ . Figure 2(a) shows these temperature profiles for various coolant-flow rates through a porous flat plate ( $Eu = 0$ ) for constant property values and zero temperature gradient at the wall, that is, for  $T_\infty/T_w = 1$  and  $\theta'_w(0) = 0$ . The values of  $n$  corresponding to the various coolant-flow rates are indicated in the figure. It can be seen in figure 2(a) that increasing the flow rate through the porous plate (i.e., increasing  $|f_w|$ ) flattens the temperature profile appreciably and increases the thickness of the temperature boundary layer. Similar profiles for stagnation flow ( $Eu = 1$ ) are shown in figure 2(b). Here, the effect of an increase in  $|f_w|$  is not nearly as pronounced as for the flat plate (fig. 2(a)). A comparison of figures 2(a) and (b) reveals the effects of Euler number on the temperature profiles for the case under consideration. Increasing the Euler number increases the temperature gradient in the boundary layer for each value of  $f_w$ , resulting in decreased thickness of the temperature boundary layer.

Figures 2(c) and (d) present temperature profiles for  $Eu = 0$  and  $Eu = 1$ , respectively, for various coolant-flow rates and both constant property values and wall temperature, that is, for  $T_\infty/T_w = 1$  and  $n = 0$ . Curves representing profiles for Prandtl numbers of 0.7 (ref. 6) and 1 and 2 (ref. 10) are also given for  $Eu = 0$ . Results for  $Pr = 1.0$  with stagnation flow ( $Eu = 1$ , fig. 2(d)) are taken from reference 2.

For flat-plate flow (fig. 2(c)) the different effect of Prandtl number for  $f_w = 0$  and  $-1$  is noteworthy. For the impermeable plate, increasing  $Pr$  steepens the temperature distribution. For the strongly

cooled plate ( $f_w = -1$ ), increasing  $Pr$  reduces the temperature near the wall. It should also be noted that in figure 2(d) the curves for  $Pr = 1$  with  $f_w = -3.1905$  and  $-4.3346$  resulted in a zero temperature gradient at the wall ( $\theta'(0) = 0$ ).

Curves for the flat-plate ( $Eu = 0$ ) and stagnation flows ( $Eu = 1$ ) are plotted in figures 2(e) and (f), respectively, for constant property values, a Prandtl number of 0.7, and a linear wall-temperature distribution ( $n = 1$ ). The effects of increased coolant flow and of increased Euler number are similar to those for a Prandtl number of 0.7 and a constant wall temperature, as shown in figures 2(c) and (d). Comparison of figures 2(c) and (e), or figures 2(d) and (f), or both shows the influence of increasing the wall-temperature-gradient parameter  $n$  from 0 to 1. An increase in the temperature gradients in the boundary layer can be observed as  $n$  increases from 0 to 1.

From the preceding discussion of figure 2, the following general trends can be noted: An increase in  $|f_w|$  results in a decrease in the temperature gradients in the boundary layer for all values of  $n$ ; an increase in  $n$  or in  $Eu$ , however, results in an increase in these temperature gradients. These increases due to wall-temperature gradient are similar to those encountered in the velocity boundary layer due to mainstream velocity gradient (see fig. 1). The velocity boundary layer is affected by velocity gradients in the mainstream (outer edge of the boundary layer); the temperature boundary layer is influenced not only by the velocity gradient but also by the temperature gradient along the wall (inner edge of the boundary layer).

Temperature profiles are given in figure 3(a) for an impermeable flat plate ( $f_w = 0$ ,  $Eu = 0$ ) of constant temperature ( $n = 0$ ) for various stream-to-wall temperature ratios (large temperature differences). Corresponding profiles for stagnation flow are shown in figure 3(b). Both figures show that increases in the stream-to-wall temperature ratio  $T_\infty/T_w$  reduce the temperature-gradient parameter  $\theta'$  in the boundary layer but have slight effect on the gradient at the wall. Euler number effects are similar to those noted in the previous figures.

The effect of variations in fluid properties and of flow through a porous wall are illustrated for a flat plate and stagnation flow in figures 3(c) and (d), respectively. For the flat plate, figure 3(c) shows that, over the range of  $\eta$  plotted, the influence of increased coolant flow through the plate exceeds that of increased temperature ratio; when  $Eu = 1$ , this situation is valid only for  $\eta < \text{about } 2.2$ .

Examples of specific-weight-flow distributions for variable property values are given in figure 4 for constant wall temperature and stagnation flow; figure 4(a) is for an impermeable wall ( $f_w = 0$ ), and figure 4(b) is for a large blowing rate ( $f_w = -1.0$ ). For these cases, overshoot

( $\frac{\rho u}{\rho_\infty U_\infty} > 1$ ) is encountered when  $T_\infty/T_w > 1$ . The maximum overshoot occurs for the permeable wall with maximum temperature ratio.

### Friction and Heat Transfer

The dimensionless skin-friction parameter  $C_{f,w}\sqrt{Re}/2$  is shown as a function of pressure-gradient parameter in figures 5 and 6 for impermeable and permeable walls. It should be recalled that for small temperature differences the velocity distributions are independent of  $n$ ; therefore, the same friction parameter will obtain for all wall-temperature variations. For large temperature differences ( $T_\infty/T_w \neq 1$ ), however, the results apply only for constant wall temperature.

The influence of  $Eu$  on the friction is quite marked, especially for  $T_\infty/T_w < 1$ . For example, when  $T_\infty/T_w = 1/4$  and  $f_w = 0$  (fig. 5), an eightfold increase in the friction results when  $Eu$  is increased from 0 to 1. Although  $T_\infty/T_w$  does not change the friction much for the flat impermeable plate, large changes are wrought for stagnation flow ( $Eu = 1$ ). (Similar results for  $Eu = 1$  are given in ref. 23. Some of the Mach number aspects in ref. 23 are discussed in ref. 24.) The curves for different temperature ratios cross at Euler number near zero. The results in figure 5 are compared with an approximate and simpler solution in reference 25 (p. 47). The approximation is poorer for  $Eu < 0$  than for  $Eu > 0$ . Larger adverse pressure gradients can be tolerated for strong cooling (i.e.,  $\frac{T_\infty}{T_w} > 1$ ) before the boundary layer separates from the wall; separation, therefore, is delayed.

Coolant-flow emission greatly reduces the friction for both small and large temperature differences (fig. 6). In contrast to the flat impermeable wall, a change in  $T_\infty/T_w$  from 1 to 4 reduces the friction by about one-third when  $f_w = -1.0$ .

Dimensionless local heat-transfer results are presented in figure 7 for small temperature differences and variable wall temperature. A particular wall-temperature variation results in a zero temperature gradient at the wall for each Euler number and coolant flow in figure 7. These values of  $n$  are given by the intercepts of the various curves with the horizontal axis and more accurately in table II.

For fixed values of  $Eu$  and  $f_w$ , increases in  $n$  yield increases in the local convective heat-transfer parameter as a result of the increased gradients in the temperature profile. Figures 7(a) and (c) show that, for a linear wall-temperature gradient (i.e.,  $n = 1$ ), a coolant flow represented approximately by  $f_w = -0.5$  is required to obtain about the same heat-transfer coefficient as for a solid wall with constant temperature.

As  $Eu$  increases from 0 to 1,  $Nu/\sqrt{Re}$  increases considerably when  $n$  and  $f_w$  are fixed. Exceptions can be noted, however. The curves for stagnation flow ( $Eu = 1$ ) and a cooled wall ( $f_w = -0.5$  and  $-1.0$ ) are essentially the same as the corresponding curves for  $Eu = 0.5$ . This similarity emphasizes that the primary pressure-gradient effects occur as  $Eu$  changes from 0 to 0.5.

In figure 8 the dimensionless local heat-transfer parameter is plotted against the Euler number for large temperature differences and a constant-temperature wall. The curves group themselves according to the coolant-flow rates considered, maximum coolant flow yielding minimum heat transfer. These curves indicate the inadvisability of increasing the coolant flow much more than that represented by a value of  $f_w$  of  $-1.0$ . Reductions in heat transfer accompany increases in temperature ratio  $T_\infty/T_w$ ; these reductions are especially marked when the wall is porous. Comparison of figures 5 and 8 shows that both friction and heat transfer are affected more by temperature ratio for stagnation flow than for flat-plate flow.

Heat-transfer results are shown in figure 9 for fluids with different Prandtl numbers and small temperature differences flowing over permeable and impermeable, isothermal flat plates ( $n = 0 = Eu$ ). Prandtl number ranges for several fluids are indicated along the abscissa. The results are converted from those given by Mickley and associates (ref. 10), by Eckert (refs. 2 and 8), and by Pohlhausen (ref. 7). There is good agreement between the present results, those of reference 2, and the comparable results of Mickley for  $f_w < 0$ . Common values are also obtained by the investigators for  $f_w = 0$  when calculations were made for identical Prandtl numbers.

The formula of Pohlhausen

$$\frac{Nu}{\sqrt{Re}} = 0.332 (Pr)^{1/3}$$

is indicated on figure 9 and shows good agreement with the results when  $f_w = 0$ . When  $f_w < 0$ , the results do not follow a simple power law. For  $f_w > 0$  the heat transfer is increased; for  $f_w < 0$  the heat transfer is

3791

3-3

decreased, as already shown in figures 7 and 8 for  $Pr = 0.7$ . Reference 6 notes that the heat transfer is the same for  $f_w = -0.5$  when  $Pr$  is 0.7 and 1.0. From figure 9 it may be concluded that this similarity holds quite well for  $0.6 \leq Pr < 1.5$ . The marked reduction in heat transfer with coolant emission is especially striking at the higher Prandtl numbers. At a Prandtl number of 5.0,  $Nu/\sqrt{Re}$  is reduced by the ratio  $1/8250$  when  $f_w$  changes from 0 to -1. This behavior may be due to the increased heat capacity of fluids with larger Prandtl numbers. In contrast to results for the impermeable plate, the heat transfer decreases with increasing Prandtl number when  $f_w < 0$ . (The case  $f_w = -0.5$  is exceptional over part of the range.)

#### SUMMARY OF RESULTS

Solutions of the laminar-boundary-layer equations were summarized for ranges of mainstream pressure gradient and rates of coolant emission through a porous wall. For small differences between the wall and stream temperature, the wall temperature was allowed to be either constant or variable; for large differences between stream and wall temperature only a constant wall temperature was considered. Solutions obtained herein were restricted to a Prandtl number at the wall of 0.7 and negligible temperature changes caused by compression and frictional heating compared with the difference between the wall and mainstream temperatures. Dimensionless forms of heat-transfer and friction parameters and boundary-layer thicknesses are tabulated.

The results of this analytical study are summarized as follows:

1. The velocity and temperature distributions near the wall indicated reduced gradients for increasing coolant emission and for increasing ratio of stream-to-wall temperature. These gradients increased for increasing mainstream pressure gradients. For small temperature differences between wall and stream, the velocity gradients are unaffected but the temperature gradients are increased by increasing wall-temperature gradient.

2. For stagnation flow over an impermeable wall, the boundary-layer velocity exceeded the mainstream velocity for stream-to-wall temperature ratios less than 1. For stream-to-wall temperature ratios greater than 1, the specific weight flow in the boundary layer exceeded that in the mainstream for stagnation flow over either a permeable or an impermeable wall.

3. Stream-to-wall temperature ratios above 1 and coolant emission diminished the friction. This effect was more marked for stagnation flow than for flat-plate flow.

4. Increased convective heat transfer accompanied larger wall temperature gradients. The heat transfer was reduced, however, by coolant

emission through the wall. These results are applicable for flat-plate and stagnation flows with small temperature differences (constant property values). For large temperature differences and a constant wall temperature, the heat-transfer parameter was reduced for increasing stream-to-wall temperature ratios. This effect is especially pronounced when the wall is porous.

5. Results were found in the literature for flow of different fluids with small temperature differences along permeable and impermeable isothermal flat plates. These results indicated much greater reductions in heat transfer due to coolant flow for Prandtl number of the order of 5 than for Prandtl number of the order of 0.7. In contrast to results for the impermeable plate, the heat transfer decreased with increasing Prandtl number and transpiration cooling.

Lewis Flight Propulsion Laboratory  
National Advisory Committee for Aeronautics  
Cleveland, Ohio, October 11, 1955

#### REFERENCES

1. Eckert, E., and Drewitz, O.: Calculation of the Temperature Field in the Laminar Boundary Layer of an Unheated Body in a High Speed Flow. R. T. P. Trans. No. 1594, British M. A. P.
2. Eckert, E. R. G.: Heat Transfer and Temperature Profiles in Laminar Boundary Layers on a Sweat-Cooled Wall. Tech. Rep. No. 5646, Air Materiel Command, Nov. 3, 1947.
3. Brown, W. Byron: Exact Solution of the Laminar Boundary Layer Equations for a Porous Plate with Variable Fluid Properties and a Pressure Gradient in the Main Stream. A.S.M.E. Proc. First U. S. Nat. Cong. Appl. Mech., publ. by A.S.M.E., 1952, pp. 843-852.
4. Brown, W. Byron, and Donoughe, Patrick L.: Tables of Exact Laminar-Boundary-Layer Solutions When the Wall is Porous and Fluid Properties are Variable. NACA TN 2479, 1951.
5. Brown, W. Byron, and Livingood, John N. B.: Solutions of Laminar-Boundary-Layer Equations Which Result in Specific-Weight-Flow Profiles Locally Exceeding Free-Stream Values. NACA TN 2800, 1952.
6. Donoughe, Patrick L., and Livingood, John N. B.: Exact Solutions of Laminar-Boundary-Layer Equations with Constant Property Values for Porous Wall with Variable Temperature. NACA TN 3151, 1954.

1675

CV-3 back

7. Pohlhausen, E.: Der Wärmeaustausch zwischen festen Körpern und Flüssigkeiten mit kleiner Reibung und kleiner Wärmeleitung. Z.a.M.M., Bd. 1, Heft 2, 1921, pp. 115-121.
8. Eckert, E.: Die Berechnung des Wärmeübergangs in der laminaren Grenzschicht umströmter Körper. VDI Forschungsheft 416, Bd. 13, Sept. und Okt., 1942. (Available from CADO as ATI 43691.)
9. Tifford, Arthur N., and Chu, Sheng To: Heat Transfer and Frictional Effects in Laminar Boundary Layers. Pt. I. "Wedge" Analyses. WADC Tech. Rep. 53-288, Wright Air Dev. Center, Wright-Patterson Air Force Base, May 1953. (Contract No. AF 33(038)-10834.)
10. Mickley, H. S., Ross, R. C., Squyers, A. L., and Stewart, W. E.: Heat, Mass, and Momentum Transfer for Flow over a Flat Plate with Blowing or Suction. NACA TN 3208, 1954.
11. Eckert, E. R. G., and Livingood, John N. B.: Method for Calculation of Laminar Heat Transfer in Air Flow Around Cylinders of Arbitrary Cross Section (Including Large Temperature Differences and Transpiration Cooling). NACA Rep. 1118, 1953. (Supersedes NACA TN 2733.)
12. Staniforth, R.: Contributions to the Theory of Effusion Cooling of Gas Turbine Blades. Paper presented at the General Discussion on Heat Transfer. Inst. Mech. Eng. (London) and A.S.M.E. (New York) Conference (London), Sept. 11-13, 1951.
13. Livingood, J. N. B., and Eckert, E. R. G.: Calculation of Transpiration-Cooled Gas-Turbine Blades. Trans. A.S.M.E., vol. 75, no. 7, Oct. 1953, pp. 1271-1278.
14. Brown, W. Byron, and Donoughe, Patrick L.: Extension of Boundary-Layer Heat-Transfer Theory to Cooled Turbine Blades. NACA RM E50F02, 1950.
15. Falkner, V. M., and Skan, Sylvia W.: Some Approximate Solutions of the Boundary Layer Equations. R. & M. No. 1314, British A.R.C., Apr. 1930.
16. Fage, A., and Falkner, V. M.: On the Relation between Heat Transfer and Surface Friction for Laminar Flow. R. & M. No. 1408, British A.R.C., Apr. 1931.
17. Schuh, H.: Laminar Heat Transfer in Boundary Layers at High Velocities. Rep. and Trans. 810, British M.A.P., Apr. 15, 1947.

18. Levy, Solomon: Heat Transfer to Constant-Property Laminar Boundary-Layer Flows with Power-Function Free-Stream Velocity and Wall-Temperature Variations. Jour. Aero. Sci., vol. 19, no. 5, May 1952, pp. 341-348.
19. Keenan, Joseph H., and Kaye, Joseph: Gas Tables. John Wiley & Sons, Inc., 1948, p. 34.
20. Emmons, H. W., and Leigh, D.: Tabulation of the Blasius Function with Blowing and Suction. Interim Tech. Rep. No. 9, Combustion Aero. Lab., Div. Appl. Sci., Harvard Univ., Nov. 1953. (Army Ord. Dept. Contract No. DA-19-020-ORD-1029.)
21. Schlichting, Hermann, und Bussmann, Karl: Exakte Lösungen für die laminare Grenzschicht mit Absaugung und Ausblasen. Schriften d. D. Akad. Luftfahrtforschung, Bd. 7B, Heft 2, 1943.
22. Tetervin, Neal, and Levine, David A.: A Study of the Stability of the Laminar Boundary Layer as Affected by Changes in the Boundary-Layer Thickness in Regions of Pressure Gradient and Flow Through the Surface. NACA TN 2752, 1952.
23. Levy, Solomon: Effect of Large Temperature Changes (Including Viscous Heating) upon Laminar Boundary Layers with Variable Free-Stream Velocity. Jour. Aero. Sci., vol. 21, no. 7, July 1954, pp. 459-474.
24. Reshotko, Eli, and Cohen, Clarence B.: Note on the Compressible Laminar Boundary Layer with Heat Transfer and Pressure Gradient. Jour. Aero. Sci., vol. 22, no. 8, Aug. 1955, pp. 584-585.
25. Thurston, Robert N.: Heat Transfer and Frictional Effects in Laminar Boundary Layers. Pt. 6. Effect of Variable Properties. WADC Tech. Rep. 53-288, Wright Air Dev. Center, Wright-Patterson Air Force Base, Sept. 1953. (Contract No. AF 33(038)-10834.)

TABLE I. - LAMINAR-BOUNDARY-LAYER SOLUTIONS

Investigator	Ref.	Type of solution	Pressure gradient	Prandtl number	Wall temperature	Type wall	Property variation
Pohlhausen	7	Exact	No	$0.7 \leq Pr \leq 15$	Constant	Impermeable	Constant
Falkner and Skan	15	Exact	Yes	----	----	Impermeable	Constant
Fage and Falkner	16	Exact	Yes	0.77	Variable	Impermeable	Constant
Eckert and Drewitz	1	Exact	Yes	0.7	Constant	Impermeable	Constant
Eckert	8	Exact and approx.	Yes	$0.6 \leq Pr \leq 10$	Constant	Impermeable	Constant
Schlichting and Bussmann	21	Exact	Yes	----	----	Permeable	Constant
Schuh	17	Exact and approx.	Yes	0.7	Variable	Impermeable	Constant
Eckert	2	Exact	Yes	1.0	Constant	Permeable	Constant
Brown and Donoughe	14	Exact	Yes	$0.6 \leq Pr \leq 1.1$	Constant	Impermeable	Constant
Brown	3	Exact	Yes	0.7	Constant	Permeable	Variable
Brown and Donoughe	4	Exact	Yes	0.7	Constant	Permeable	Variable
Staniforth	12	Approx.	Yes	0.71	Constant	Permeable	Constant
Brown and Livingood	5	Exact	Yes	0.7	Constant	Permeable	Variable
Levy	18	Exact	Yes	$0.7 \leq Pr \leq 20$	Variable	Impermeable	Constant
Eckert and Livingood	11	Approx.	Yes	0.7	Constant	Permeable	Variable
Eckert and Livingood	13	Approx.	Yes	0.7	Constant	Permeable	Variable
Tifford and Chu <sup>a</sup>	9	Exact	Yes	$0.5 \leq Pr \leq 10$	Variable	Impermeable	Variable
Emmons and Leigh	20	Exact	No	----	----	Permeable	Constant
Thurston <sup>a</sup>	25	Approx.	Yes	0.7 & 1.0	Constant	Impermeable	Variable
Donoughe and Livingood	6	Exact	Yes	0.7	Variable	Permeable	Constant
Mickley	10	Exact	No	$0.6 \leq Pr \leq 5.0$	Constant	Permeable	Constant
Levy	23	Exact	Yes	0.7 & 1.0	Constant	Impermeable	Variable

<sup>a</sup>Summary report.

TABLE II. - SUMMARY OF HEAT-TRANSFER AND FRICTION PARAMETERS AND BOUNDARY-LAYER THICKNESSES

(a) Small temperature differences  $\frac{T_{\infty}}{T_w} = 1$

$f_w$	Eu	n	$\frac{Nu}{\sqrt{Re}}$	$\frac{C_{f,w}\sqrt{Re}}{2}$	$\frac{\delta^*\sqrt{Re}}{x}$	$\frac{\delta_1\sqrt{Re}}{x}$	$\frac{\delta_c\sqrt{Re}}{x}$	$\frac{\delta_t\sqrt{Re}}{x}$	Additional information	
									Reference	Page
0	-0.0904	0	0.1993	0	3.498	0.868	0.626	2.737	4	11
	-.0868	0	.2215	.0581	2.971	.852	.692	2.505	↓	↓
	-.0826	0	.2310	.0870	2.763	.838	.720	2.415	↓	↓
	-.0741	0	.2435	.1296	2.510	.812	.752	2.307	4	12
	-.0654	0	.2528	.1637	2.336	.788	.773	2.233	↓	↓
	-.0476	0	.2673	.2202	2.092	.747	.801	2.128	↓	↓
	0	-0.500	0	0.3320	1.7215	0.665	1.861	3.417	6	24
	0	0	.2927	↓	↓	↓	.835	1.959	4,6	13,24
	0	.500	.4059	↓	↓	↓	.578	1.562	6	24
	0	1.000	.4803	↓	↓	↓	.458	1.363	6	24
	0.5	-0.750	0	0.8998	0.854	0.377	1.6075	2.403	6	25
	0	0	.4162	↓	↓	↓	.792	1.407	4,6	14,25
0	.500	.5426	↓	↓	↓	.620	1.186	6	25	
0	1.000	.6350	↓	↓	↓	.518	1.0515	6	25	
1.000	-1.000	0	1.2326	0.648	0.292	1.409	2.0175	6	26	
0	-.500	.3228	↓	↓	↓	.9185	1.440	6	26	
0	0	.4958	↓	↓	↓	.708	1.187	4,6	15,26	
0	.500	.6159	↓	↓	↓	.586	1.036	6	26	
0	1.000	.7090	↓	↓	↓	.506	.936	6	26	
-0.5	-0.0418	0	0.1029	0	4.272	0.954	0.807	3.677	4	28
	0	-0.3702	0	0.1645	2.4595	0.829	1.921	4.134	6	27
	0	0	.1661	↓	↓	↓	.974	2.6495	4,6	29,27
	0	.500	.2611	↓	↓	↓	.623	2.047	6	27
	0	1.000	.3211	↓	↓	↓	.472	1.763	6	27
	0.5	-0.5356	0	0.6974	1.034	0.444	1.743	2.706	6	28
	0	-.500	.0272	↓	↓	↓	1.651	2.593	6	28
	0	0	.2594	↓	↓	↓	.994	1.776	4,6	30,28
	0	.500	.3834	↓	↓	↓	.738	1.445	6	28
	0	1.000	.4711	↓	↓	↓	.599	1.258	6	28
	1.0	-0.6789	0	0.9692	0.7805	0.344	1.5535	2.288	6	29
	0	0	.2934	↓	↓	↓	.918	1.530	4,6	31,29
0	.500	.4132	↓	↓	↓	.7265	1.292	6	29	
0	1.000	.5030	↓	↓	↓	.609	1.145	6	29	
-1.0	-0.0072	0	0.0251	0	6.398	1.116	1.072	5.997	4	39
	0	-0.2384	0	0.0355	4.392	1.072	1.909	5.860	6	30
	0	0	.0516	↓	↓	↓	1.150	4.414	4,6	40,30
	0	.500	.1052	↓	↓	↓	.650	3.338	6	30
	0	1.000	.1383	↓	↓	↓	.465	2.871	6	30
	0.05	0	0.0881	0.1410	2.796	0.911	1.241	3.317	4	41
	0	0	.1129	.2703	2.008	.750	1.280	2.806	4	42
	0.50	-0.3585	0	0.5345	1.260	0.523	1.905	3.078	6	31
	0	0	.1392	↓	↓	↓	1.270	2.274	4,6	43,31
	0	.500	.2528	↓	↓	↓	.889	1.783	6	31
	0	1.000	.3314	↓	↓	↓	.700	1.524	6	31
	1.0	-0.4235	0	0.7565	0.945	0.405	1.731	2.622	6	32
0	0	.1457	↓	↓	↓	1.208	1.995	4,6	44,32	
0	.500	.2553	↓	↓	↓	.910	1.627	6	32	
0	1.000	.3360	↓	↓	↓	.740	1.411	6	32	

3791

TABLE II. - Concluded. SUMMARY OF HEAT-TRANSFER AND FRICTION PARAMETERS AND BOUNDARY-LAYER THICKNESSES

(b) Large temperature differences with constant wall temperature ( $n = 0$ )

$f_w$	$\frac{T_{\infty}}{T_w}$	Eu	$\frac{Nu}{\sqrt{Re}}$ $\theta'_w$	$\frac{C_{f,w} \sqrt{Re}}{2}$ $f_w''$	$\frac{\delta^* \sqrt{Re}}{x}$	$\frac{\delta_1 \sqrt{Re}}{x}$	$\frac{\delta_c \sqrt{Re}}{x}$	$\frac{\delta_t \sqrt{Re}}{x}$	Additional information		
									Refer- ence	Page	
0	0.25	0	0.2884	0.3556	2.031	0.182	0.246	1.482	4	62	
		.50	.4801	1.9299	1.033	-.031	.270	.919		64	
		1.00	.5812	2.7842	.820	-.064	.246	.764		65	
	0.5	-0.06	0.2062	0	3.043	0.442	0.348	2.215	4	57	
		-.04	.2554	.1735	2.309	.406	.420	1.846		58	
		0	.2900	.3462	1.898	.347	.457	1.645		59	
		.50	.4412	1.2754	.980	.116	.460	1.109		60	
		1.00	.5298	1.8000	.768	.065	.415	.929		61	
	2	-0.1178	0.1890	0	4.582	1.663	1.076	3.721	4	16	
		-.09	.2522	.1634	2.430	1.501	1.408	2.928		17	
		-.05	.2756	.2434	1.882	1.378	1.478	2.713		18	
		0	.2944	.3125	1.537	1.271	1.495	2.547		19	
.50		.4020	.6836	.622	.838	1.372	1.904	5			
1.00	.4760	.9090	.433	.693	1.215	1.611	5	19			
4	-0.1351	0.1794	0	6.950	3.109	1.834	5.596	4	22		
	-.09	.2642	.1934	2.297	2.719	2.595	4.053		23		
	-.05	.2790	.2397	1.810	2.582	2.651	3.863		24		
	0	.2952	.2874	1.438	2.455	2.663	3.678		25		
	.50	.3940	.5541	.272	1.676	2.399	2.790		5		
1.00	.4662	.7220	.081	1.403	2.113	2.370	5	25			
-0.5	2	0	0.1602	0.1476	2.381	1.605	1.778	3.456	4	32	
		.50	.2304	.4770	.772	1.044	1.771	2.476		5	20
		1.00	.2560	.6415	.507	.880	1.638	2.151		5	21
	4	-0.0644	0.0796	0	7.219	3.485	2.620	7.329	4	35	
		0	.1506	.1263	2.460	3.100	3.237	5.012		4	36
		.50	.2088	.3448	.318	2.155	3.142	3.670		5	26
1.00	.2252	.4465	0	1.867	2.932	3.233	5	27			
-1.0	2	0	0.0406	0.0242	4.931	2.114	2.167	5.941	4	45	
		.05	.0692	.0892	2.985	1.911	2.299	4.625		46	
		.15	.0886	.1678	1.989	1.704	2.343	3.959		47	
		.50	.1062	.3228	.965	1.310	2.298	3.236		5	22
		1.00	.1052	.4445	.608	1.148	2.228	2.891		5	23
	4	0	0.0262	0.0125	6.409	4.160	4.002	9.007	4	51	
		.05	.0510	.0542	3.405	3.881	4.247	6.995		52	
		.15	.0656	.1030	2.040	3.620	4.309	6.054		53	
		.50	.0780	.1959	.402	2.882	4.256	4.954		5	28
		1.00	.0726	.2611	-.117	2.602	4.147	4.448		5	29

3791

CV-4 3791

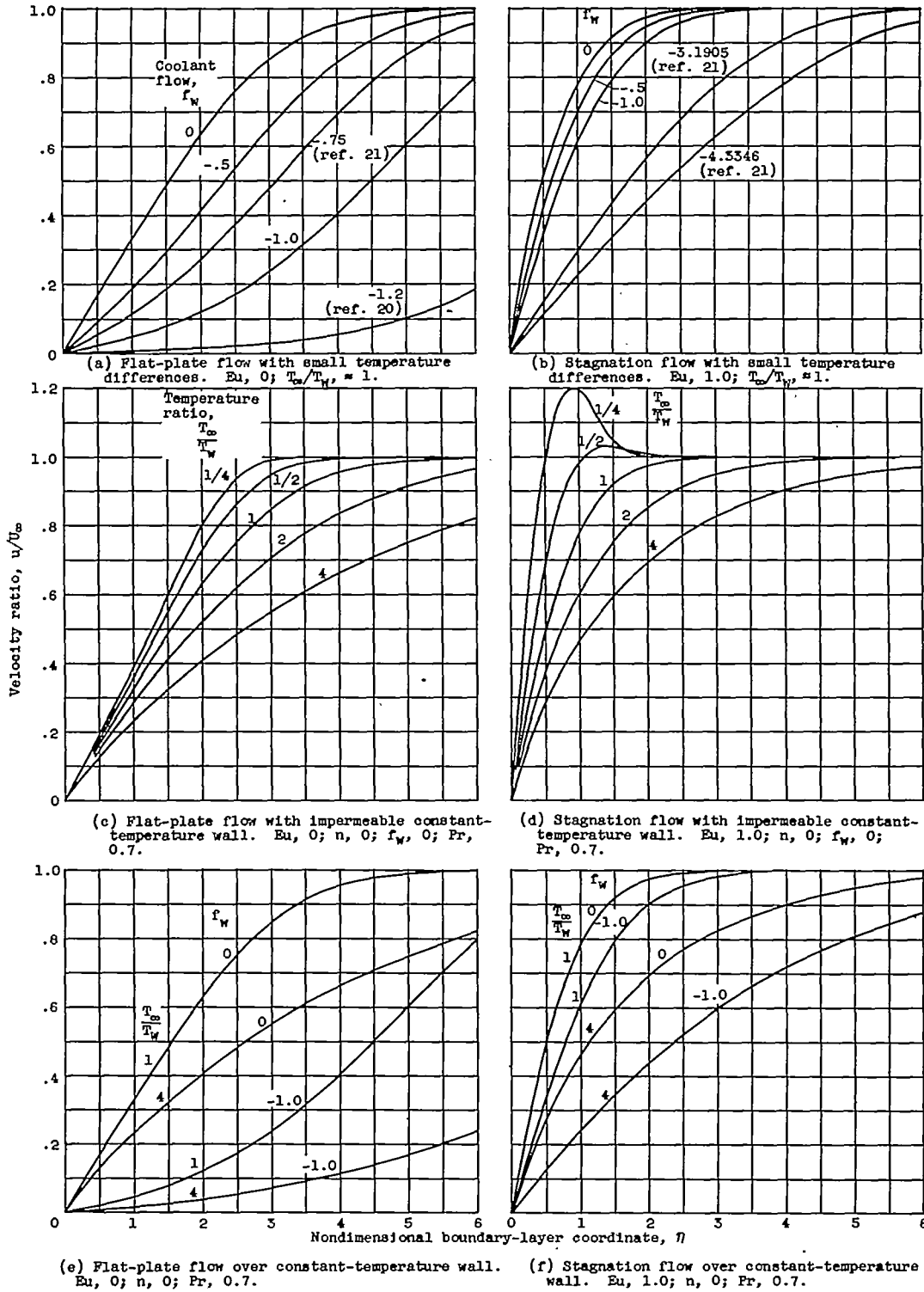


Figure 1. - Velocity distributions in laminar boundary layer.

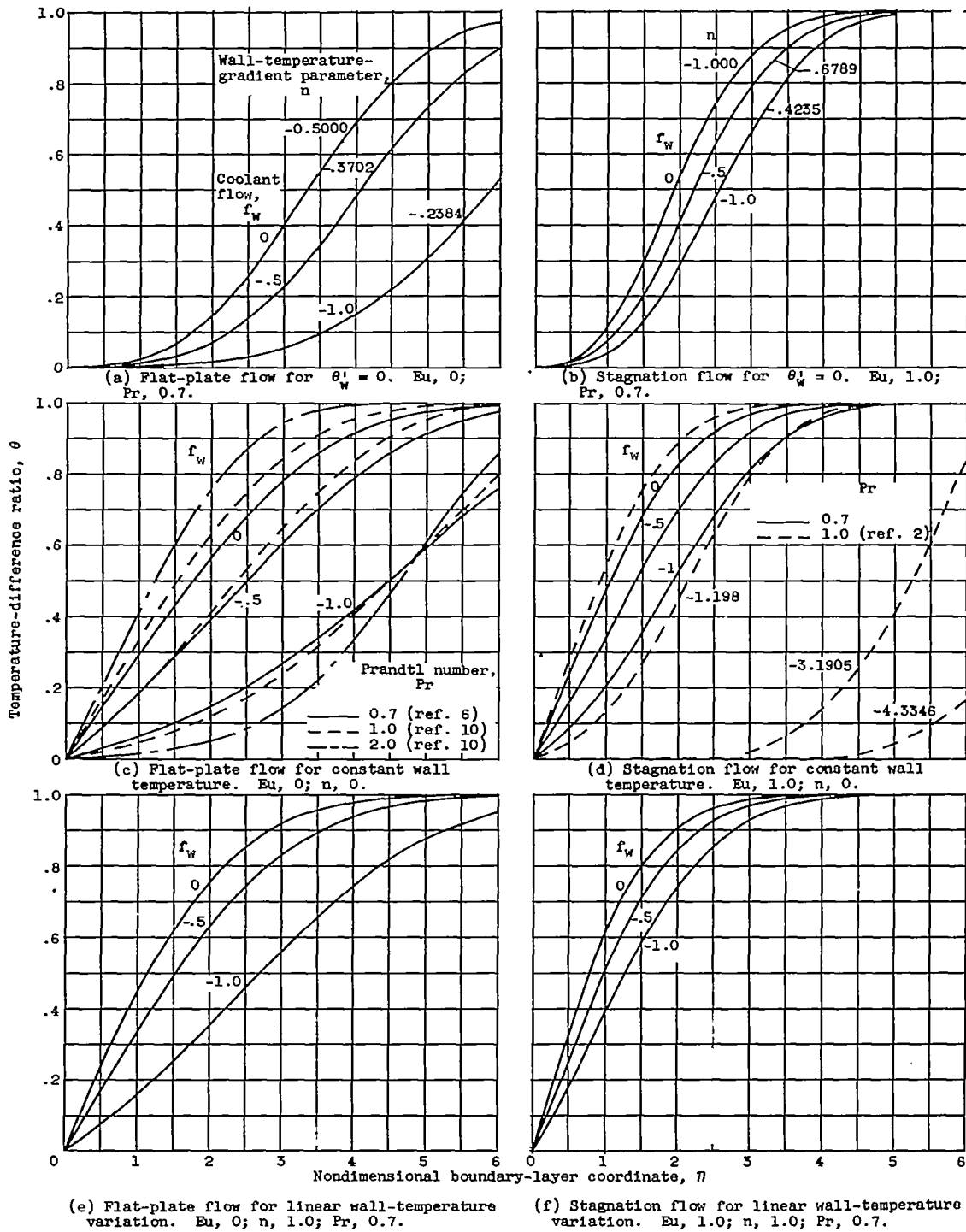


Figure 2. - Temperature distributions in laminar boundary layer with small temperature differences ( $T_\infty/T_w \approx 1$ ).

3791

CV-4 back

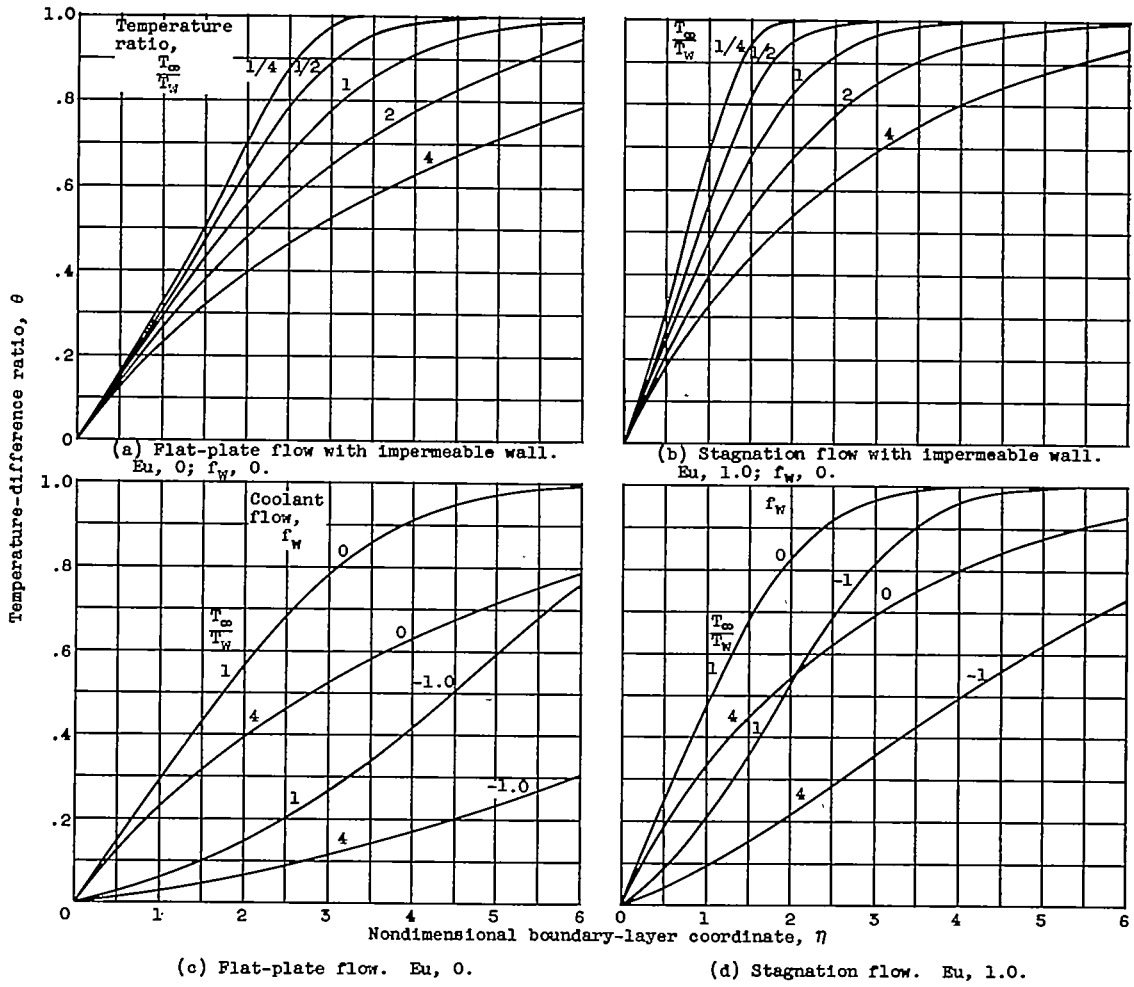
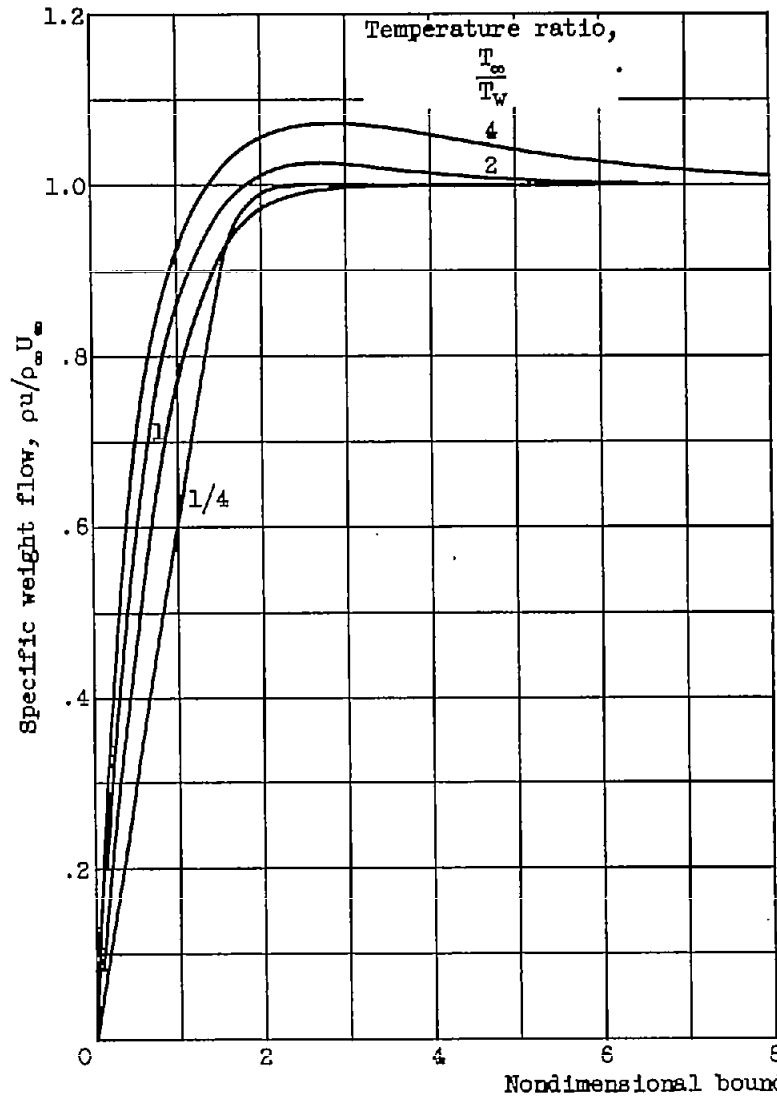
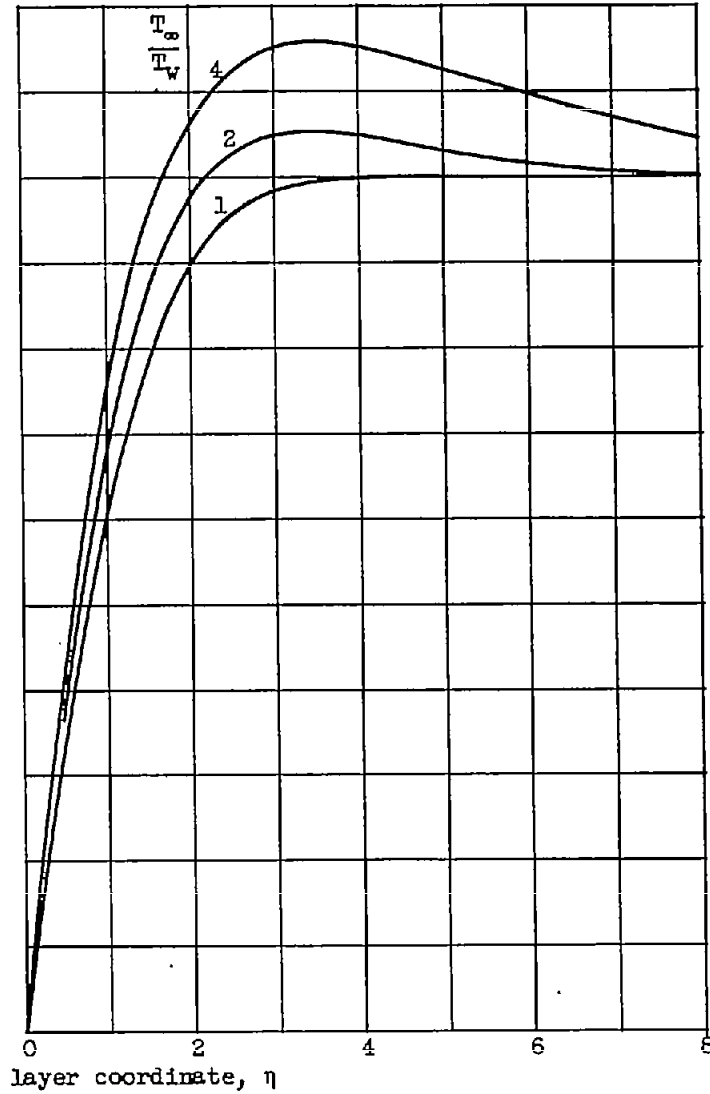


Figure 5. - Temperature distributions in laminar boundary layer for large temperature differences and constant wall temperature. Wall-temperature-gradient parameter, 0; Prandtl number, 0.7.



(a) Impermeable wall ( $f_w = 0$ ).



(b) Large blowing rate ( $f_w = -1.0$ ).

Figure 4. - Specific-weight-flow distributions in laminar boundary layer for stagnation flow with constant wall temperature. Euler number, 1.0; wall-temperature-gradient parameter, 0; Prandtl number, 0.7.

3791

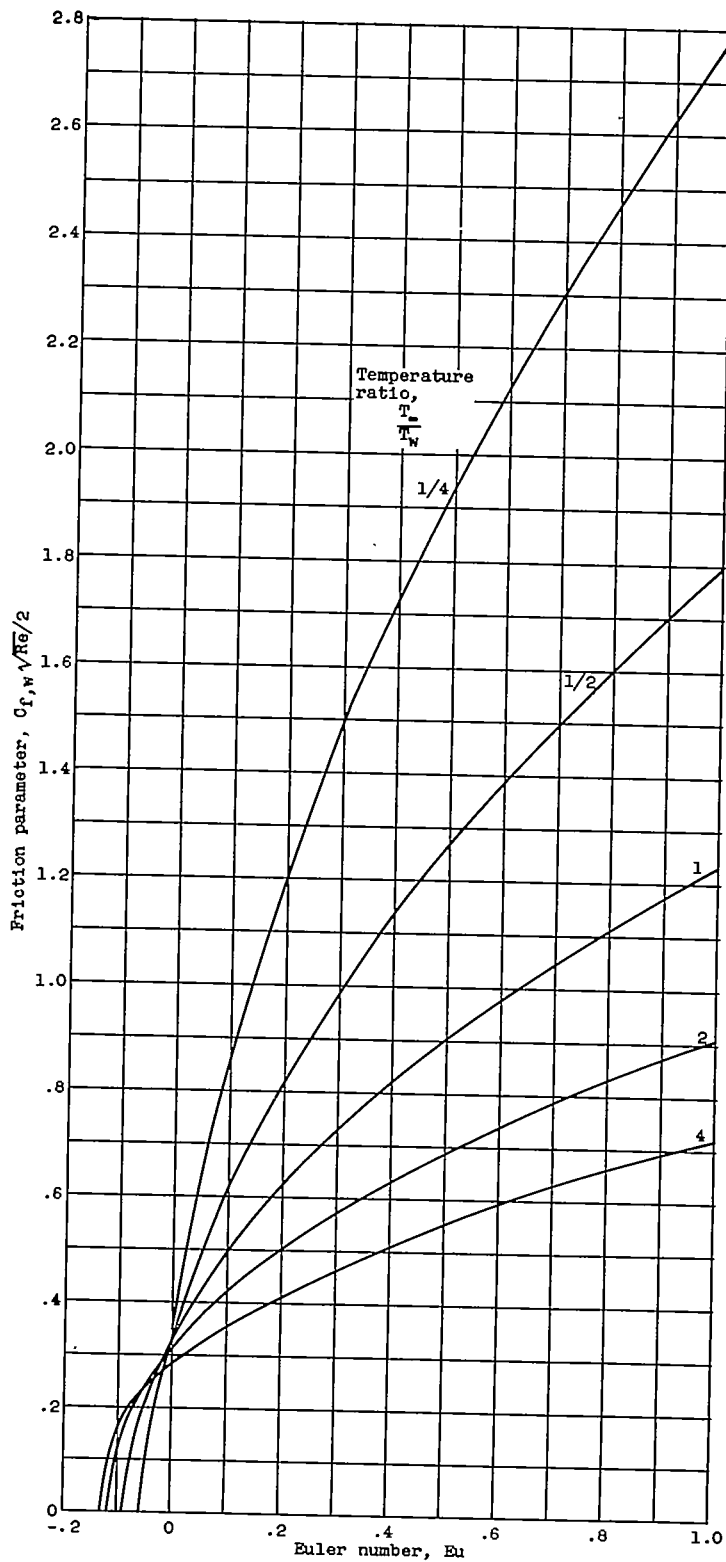


Figure 5. - Skin-friction parameter for laminar boundary layer for impermeable wall at constant temperature. Coolant flow, 0; wall-temperature-gradient parameter, 0.

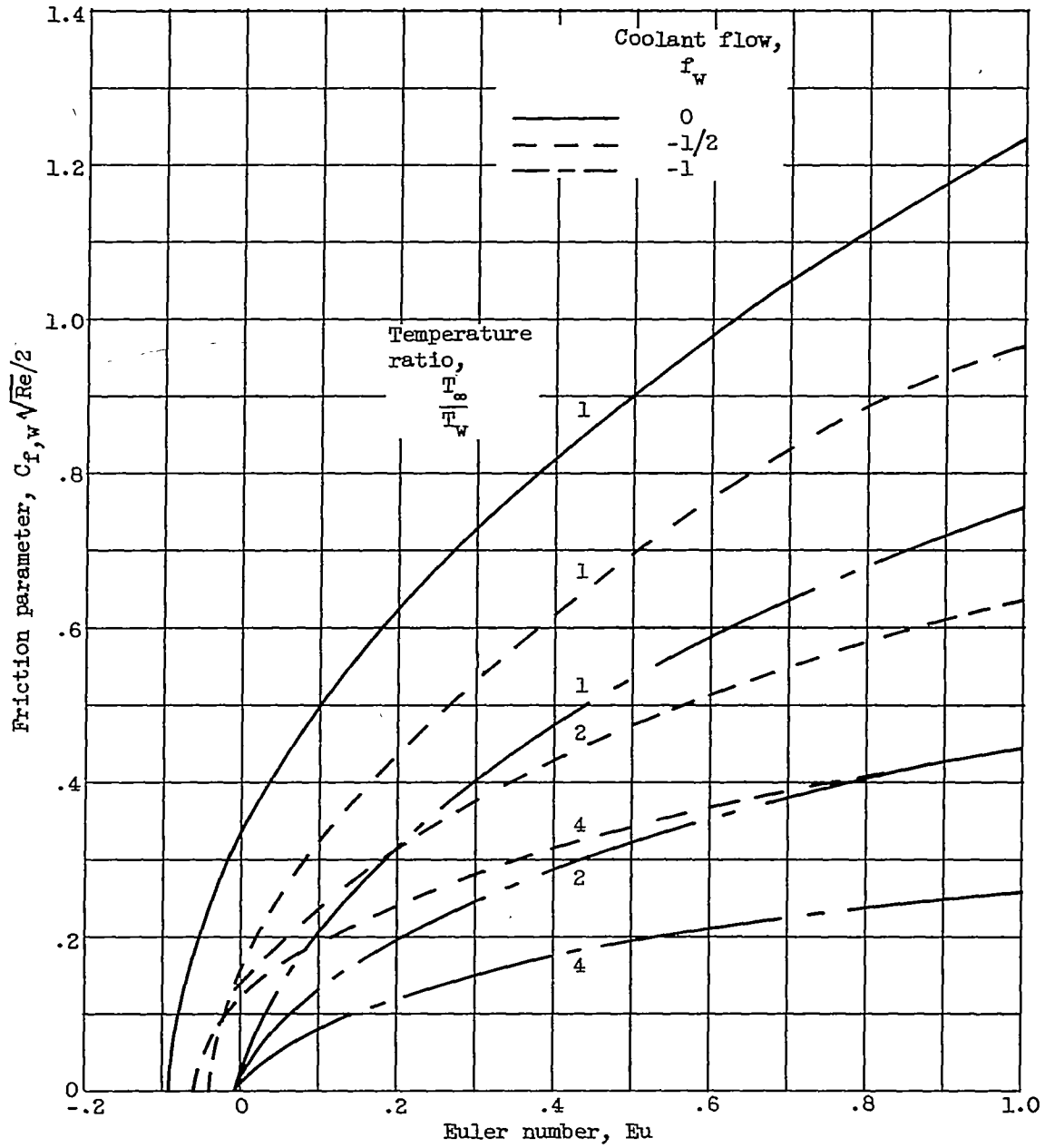


Figure 6. - Skin-friction parameter for laminar boundary layer for permeable and impermeable walls at constant temperature. Wall-temperature-gradient parameter, 0.

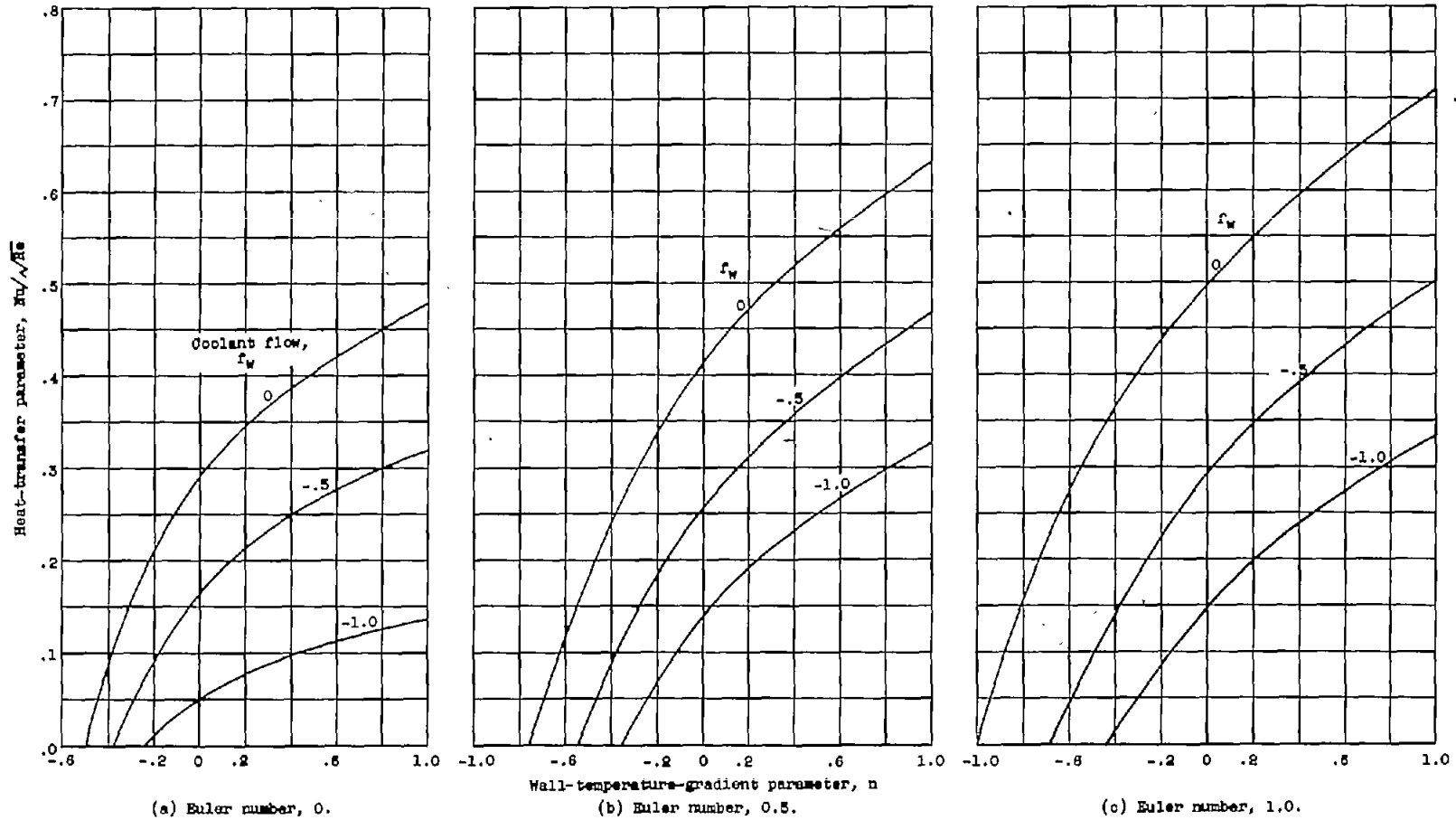


Figure 7. - Heat-transfer parameter for constant-property laminar boundary layer for permeable and impermeable walls at variable temperatures. Prandtl number, 0.7.

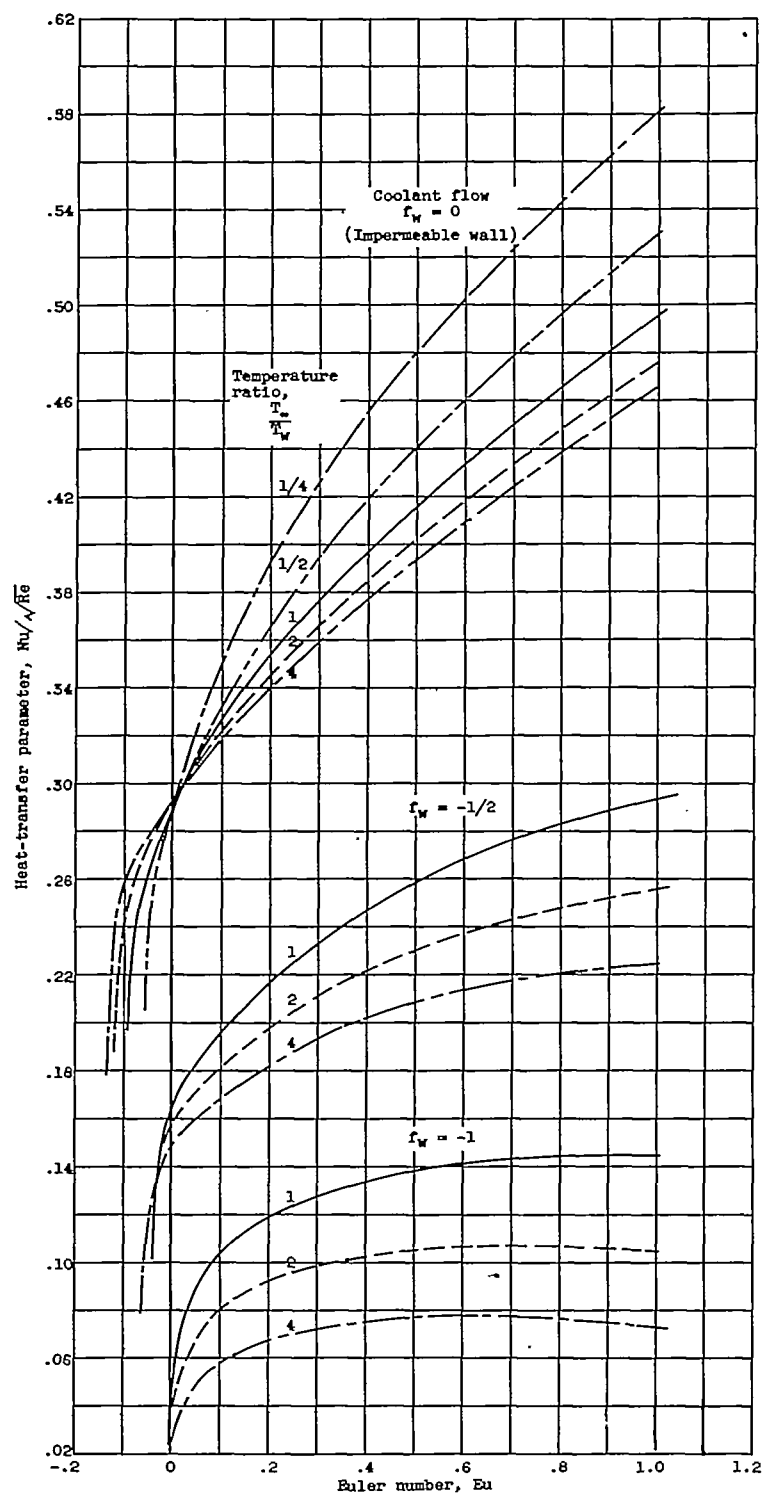


Figure 8. - Heat-transfer parameter for laminar boundary layer for permeable and impermeable walls at constant temperature. Wall-temperature-gradient parameter, 0; Prandtl number, 0.7.

3791

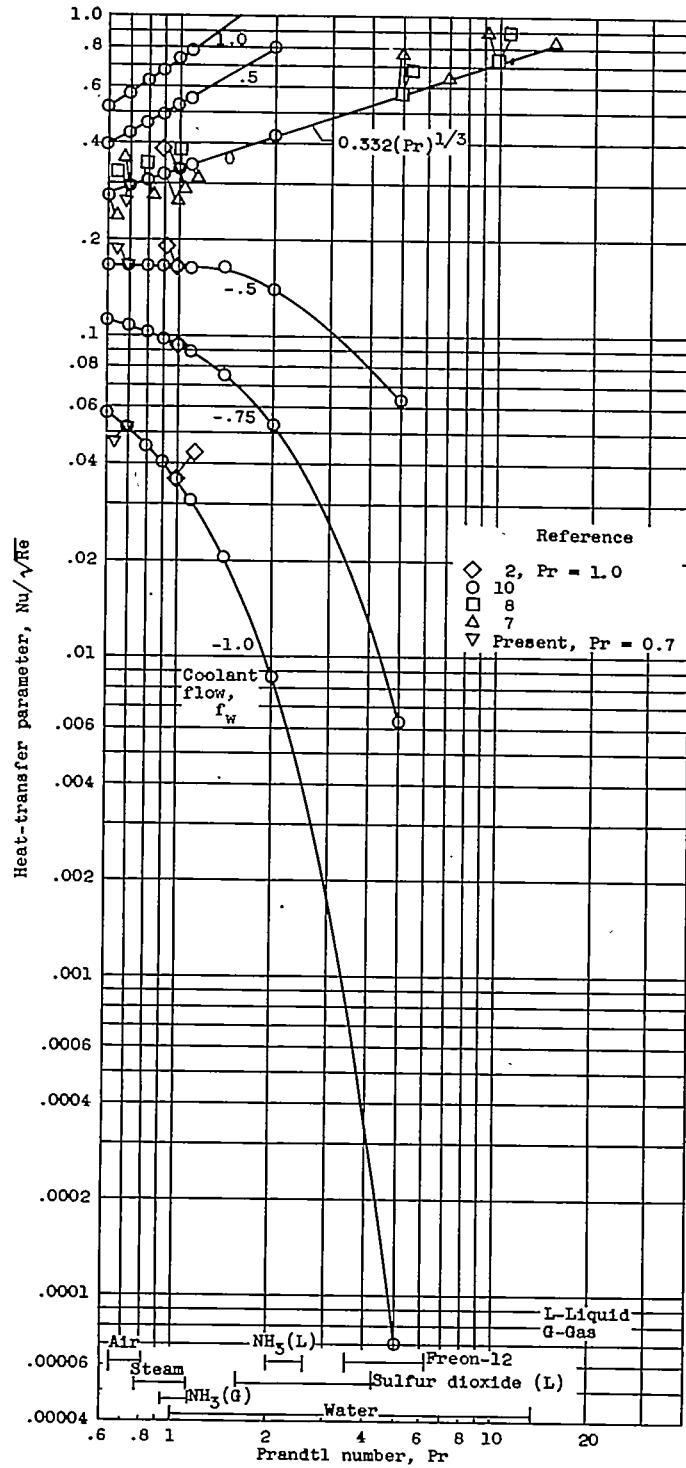


Figure 9. - Heat-transfer parameter for constant-property laminar boundary layer for different fluids. Constant wall temperature, wall-temperature-gradient parameter, 0; Euler number, 0.